AN INTER-SENSOR CALIBRATION AND ATMOSPHERIC CORRECTION SYSTEM FOR LONG-TERM TIME SERIES OF AVHRR HRPT DATA

Lihong Su, Assistant Research Scientist
James Gibeaut, Associate Research Professor
Harte Research Institute for Gulf of Mexico Studies
Texas A&M University - Corpus Christi
Corpus Christi, TX 78412
Su.Lihong@tamucc.edu
James.Gibeaut@tamucc.edu

ABSTRACT

Remotely sensed data are benefiting marine and coastal ecosystem studies. The NOAA AVHRR data series has more than 30 years of unique and valuable earth observation imagery available. These data, however, were acquired by multiple satellites and stored in multiple file formats. To use the long-term data, inter-sensor calibration and atmospheric correction are essential processing steps. After reviewing related papers and analyzing legacy processing codes, a novel architecture was designed. Portions of legacy processing codes were re-written for up-to-date computing environments and integrated with new processing codes to form an efficient system. The system can process all five HRPT (High Resolution Picture Transmission) file formats from 12 AVHRR sensors from the 1980s to the present. The system first decodes five different HRPT formats and loads data into a geodatabase for subsequent processing. It then transforms counts with an inter-sensors consistent calibration to compensate for degradation of AVHRR sensors. The counts are converted to top-of-atmosphere (TOA) radiance. The TOA radiance subsequently is converted to water-leave reflectance by eliminating Rayleigh scattering and aerosol effects. The water-leave reflectance is an important input to marine ecosystem and estuary studies. The first task of this system is to process 25 years of AVHRR data that cover three Texas estuaries from 1985 to 2010 to support investigations of changes in suspended sediments patterns in three Texas estuaries.

Keywords: AVHRR, HRPT data, estuary, coastal environments, calibration, atmospheric correction
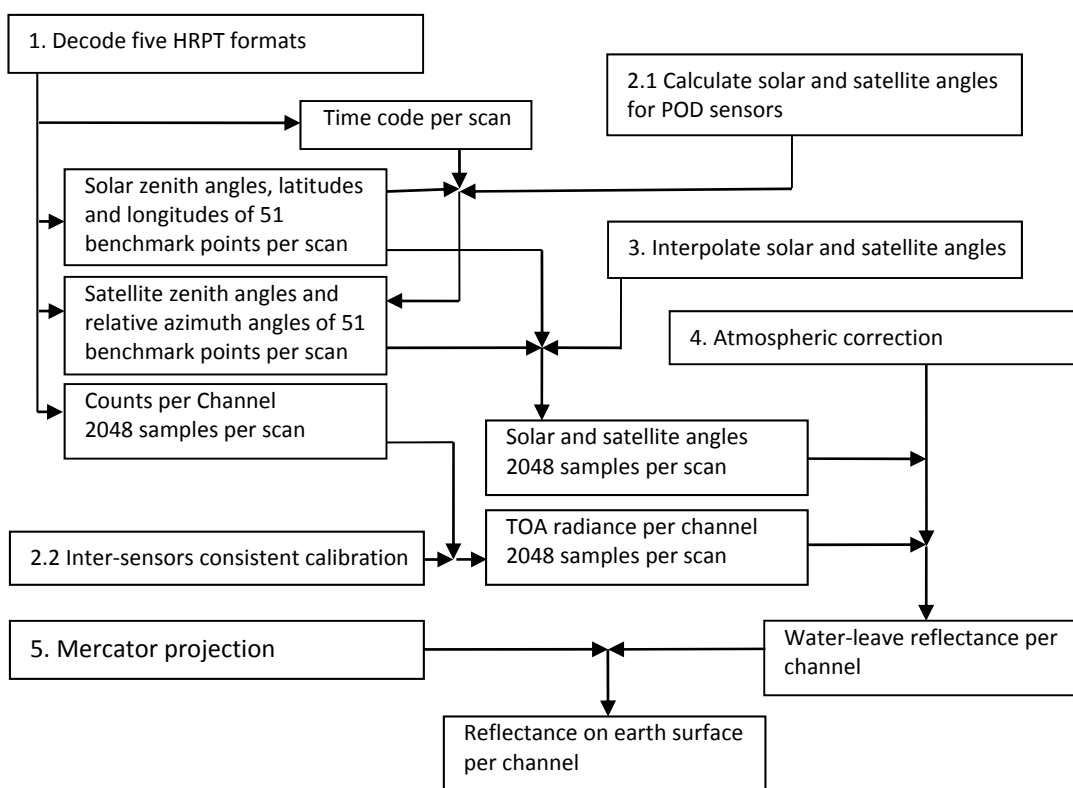
INTRODUCTION

The amount of suspended sediment plays an important role in determining the distribution of habitats in estuaries. Observations from the Advanced Very High Resolution Radiometer (AVHRR) can show daily distribution of suspended sediment concentration of surface waters across a wide area (Stumpf 1988). AVHRR imagery of 25 years from 1985 to 2010 is being used to derive a geospatial time series of the concentration of total suspended matter of the Texas bays and estuaries. To use long-term AVHRR data, inter-sensor consistent calibration is required. Similarly, atmospheric correction is essential for converting top-of-atmosphere (TOA) radiance to water-leave reflectance, which is relevant to suspended sediment concentration of surface waters. This research developed a processing system of inter-sensor calibration and atmospheric correction for long-term AVHRR imagery.

DESIGN OF THE PROCESSING SYSTEM

The AVHRR sensor began acquiring data in 1978. The normal file format of AVHRR data is called HRPT (High Resolution Picture Transmission). There are five different HRPT formats of 12 AVHRR sensors from the 1980s to present (Table 1). The system first decodes five different HRPT formats and loads data into a geodatabase. Next, the system transforms counts using an inter-sensors consistent calibration method and performs atmospheric correction. Figure 1 shows workflow of the processing system.

Sensor	HRPT format				
NA=NOAA-6	*				
NC=NOAA-7	*				
NE=NOAA-8	POD pre-Sep8,92				
NF=NOAA-9	*	*	POD post-Nov15,94		
NG=NOAA-10	*	POD between Sep8,92 and Nov15,94	*		
NH=NOAA-11	*		*		
ND=NOAA-12	*		*		
NJ=NOAA-14		*	*		
NK=NOAA-15				KLM pre-Apr28,05	post-Nov14,06
NL=NOAA-16				*	
NM=NOAA-17				*	
NN=NOAA-18					*

Flowchart:

1. Decode five HRPT formats

Time code per scan

Solar zenith angles, latitudes and longitudes of 51 benchmark points per scan

Satellite zenith angles and relative azimuth angles of 51 benchmark points per scan

Counts per Channel 2048 samples per scan

2.1 Calculate solar and satellite angles for POD sensors

3. Interpolate solar and satellite angles

4. Atmospheric correction

Solar and satellite angles 2048 samples per scan

2.2 Inter-sensors consistent calibration

TOA radiance per channel 2048 samples per scan

5. Mercator projection

Water-leave reflectance per channel

Reflectance on earth surface per channel

Figure 1. Workflow of the AVHRR data processing.

ALGORITHMS

Radiometric Calibration and Inter-Sensor Consistent Calibration

AVHRR sensors measure radiance which is converted to voltage and stored as a 10-bit digital count, which varies from 0-1023. Radiometric calibration is needed to convert the counts to radiance. Thus, a calibration factor must be determined that relates radiance to digital counts (figure 2). Inter-sensor consistent calibration is required to compensate for degradation of AVHRR sensors.

radiance → voltage → counts → calibration factor → radiance

Measured by a sensor

Calibrated by algorithms
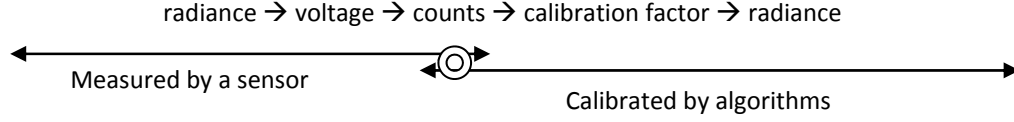
Figure 2. radiometric measurement and calibration.

Heidinger gave an approach to perform radiometric calibration and inter-sensor calibration at the same time (Heidinger, 2010). The approach, however, does not generate radiance received by a sensor. Like some researchers, who considered that the reflectance measured in an AVHRR field of view is represented by a 10-bit raw pixel count (Tahnk and Coakley, 2002), Heidinger uses

$$R_{Cal} = S * (C_{10} - C_{dark}) \qquad (1)$$

to generate a calibrated instrument reflectance. Here term C_{dark} is the dark count, which is what the instrument would measure under dark conditions. Term S is the calibration slope, which is also known as the inverse-gain. C_{10} is the AVHRR signal in 10-bit counts. Heidinger used a second order polynomial for calibrating the sensor degradation.

$$S(t) = S_0 * (100.0 + a * t + b * t^2)/100.0 \qquad (2)$$

where S_o is the calibration slope at time $t=0$ and t is the time after launch expressed in years. The values of S_0, a and b are provided by Heidinger (2010) for AVHRR sensors on the TIROS-N to Metop-A satellites.

To compensate for atmospheric effects, the instrument reflectance R_{cal} should be converted to radiance received by a sensor. The R_{cal} is related to isotropic albedo A by

$$A = \frac{\rho^2 \cdot R_{cal}}{\cos\theta_0}. \qquad (3)$$

For a diffuse surface, $A = \dfrac{\pi \cdot L_{cal}}{\dfrac{E_0}{\rho^2}\cos\theta_0}$. Thus, we have

$$\frac{\pi \cdot L_{cal}}{\dfrac{E_0}{\rho^2}\cos\theta_0} = \frac{\rho^2 \cdot R_{cal}}{\cos\theta_0} \qquad (4)$$

$$L_{cal} = \frac{E_0}{\pi} R_{cal} \qquad (5)$$

We can set $S' = \dfrac{E_0}{\pi}$. The E_0 is in-band solar irradiance. The ρ is a parameter for Earth-Sun distance. θ_o is Sun zenith angle. S' is expressed in units of W (m^{-2} sr^{-1} μm^{-1} count^{-1}). The L_{cal} is in-band upwelling radiance in W/(m^2 sr μm) received by AVHRR sensors. It also can be written as $L_{upwelling}$ or L_{sensor}. The $\dfrac{E_0}{\pi}$ is constant for a given AVHRR channel. Finally, Equation 6 is used to convert a count to an in-band upwelling radiance at the top of the atmosphere for the 12 AVHRR sensors from 1985 to 2010.

$$L_{cal} = \frac{E_0}{\pi} \cdot (C_{10} - C_{dark}) \cdot S_0 \cdot (100.0 + a \cdot t + b \cdot t^2)/100.0 \qquad (6)$$

Atmospheric Correction

The legacy FORTRAN codes (Stumpf personal communication) were used to startup the atmospheric correction. Part these codes were renovated to C#.NET. Based on analysis of these legacy codes and review of related literatures (Gordon and Castano, 1987; Stumpf, 1988; Gordon and Castano, 1987; Stumpf and Pennock, 1989), a complete derivation of equations for atmospheric correction is given below for the first time.

The algorithm is most easily understood and applied to imagery by considering first only single scattering. In this approximation, assuming that the sea surface is flat, water reflectance (R) is determined as

$$R(\lambda) = \frac{\pi \cdot L_{water}(\lambda)}{F_0(\lambda) \cos\theta_0 e^{-(\tau_{Rayleigh}/2 + \tau_{Oz})/\cos\theta_0}} \qquad (7)$$

where λ is the wavelength. θ_0 is the solar zenith angle. Transmission losses of the incident solar irradiance are accounted for by the exponential term, wherein $\tau_{Rayleigh}(\lambda)$ is the optical thickness for Rayleigh scattering and $\tau_{Oz}(\lambda)$ is the ozone optical thickness.

F_0 is the solar irradiance at the top of the atmosphere. Because the earth's orbit is slightly elliptical, the intensity of solar radiation received outside the earth's atmosphere varies as the square of the earth-sun distance. This variation may be approximated by:

$$F_0 = \frac{E_0}{\rho^2} = E_0 \left[1 + 0.033412 \cdot \cos\left(2\pi\frac{\text{Julian\_day} - 3}{365.25}\right)\right] = E_0 \cdot \delta_{ES} \ (\text{W/m}^2) \qquad (8)$$

E_0 is the solar constant, which depends on wavelength. Every sensor has its band width and spectral response function. For example, NOAA-12 has spectral band widths 0.58-0.68 and 0.725-1.10 micrometers for channels 1 and 2. The solar irradiance should be integrated over the spectral response of AVHRR sensors. For NOAA-12, the integrated solar spectral irradiance of channels 1 and 2 is 200.1 and 229.9 W/m². Further, the equivalent width of the spectral response functions of channels 1 and 2 is 0.124 and 0.219 μm (Table 3.3.2-2 on website http://www.ncdc.noaa.gov/oa/pod-guide). So for NOAA-12, the solar constant is 1614 and 1050 W/(m²μm) for channels 1 and 2. δ_{ES} is a correction factor for the earth-sun distance.

L_{water} is water-leaving radiance (in W/(m²μm·sr)) from the water column. L_{water} can be found from the radiance received at the sensor (L_{sensor}) using

$$L_{water}(\lambda) = \frac{L_{sensor}(\lambda) - L_{path}(\lambda)}{T_1(\lambda)} - L_{gl\,int}(\lambda) \qquad (9)$$

where L_{sensor} can be obtained via method described in Section 3.1. L_{glint} is the radiance reflected from the water surface (i.e. sun glint). Outside of regions containing sun glint, L_{glint} can be ignored. L_{path} is the atmospheric path radiance. T_1 is the atmospheric diffuse transmission coefficient from the Earth to the satellite.

$$T_1(\lambda) = e^{-(\tau_{aerosol} + \tau_{Rayleigh}/2 + \tau_{Oz})/\cos\theta} \qquad (10)$$

where $\tau_{aerosol}$ is found from a linear relationship to $L_{aerosol}$. L_{path} can be found from

$$L_{path}(\lambda) = L_{Rayleigh}(\lambda) + L_{aerosol}(\lambda) \qquad (11)$$

where $L_{Rayleigh}$ is the Rayleigh radiance and $L_{aerosol}$ is the aerosol (haze) radiance. Now let $L_{aerosol}$ be zero (Stumpf's codes) and consider only $L_{Rayleigh}$. The aerosol effect will be reduced later.

Thus, $R(\lambda)$ is written by

$$R(\lambda) = \frac{\pi \cdot (L_{sensor}(\lambda) - L_{Rayleigh}(\lambda))}{E_0(\lambda)\delta_{ES} \cos\theta_0 e^{-(\tau_{Rayleigh}/2 + \tau_{Oz})/\cos\theta_0} e^{-(\tau_{Rayleigh}/2 + \tau_{Oz})/\cos\theta}} \qquad (12)$$

$$= \frac{\pi \cdot \left(L_{sensor}(\lambda) - L_{Rayleigh}(\lambda)\right)}{E_0(\lambda)\delta_{ES}\cos\theta_0 \, e^{-\left(\frac{\tau_{Rayleigh}}{2} + \tau_{Oz}\right)\left(\frac{1}{\cos\theta_0} + \frac{1}{\cos\theta}\right)}} \tag{13}$$

$$= \frac{1}{e^{-\left(\frac{\tau_{Rayleigh}}{2} + \tau_{Oz}\right)\left(\frac{1}{\cos\theta_0} + \frac{1}{\cos\theta}\right)}} \left[\frac{\pi \cdot L_{sensor}(\lambda)}{E_0(\lambda)\delta_{ES}\cos\theta_0} - \frac{\pi \cdot L_{Rayleigh}(\lambda)}{E_0(\lambda)\delta_{ES}\cos\theta_0}\right] \tag{14}$$

Here $e^{-\left(\frac{\tau_{Rayleigh}}{2} + \tau_{Oz}\right)\left(\frac{1}{\cos\theta} + \frac{1}{\cos\theta_0}\right)}$ is the diffuse transmittance of the atmosphere on two trips between the sea surface and the sensor, and between the sea surface and the sun.

The Rayleigh radiance $L_{Rayleigh}$ is given by

$$L_{Rayleigh}(\lambda) = \omega_{Rayleigh}(\lambda)\tau_{Rayleigh}(\lambda)F_0'(\lambda)p_{Rayleigh}(\theta,\theta_0,\lambda)/4\pi\cos\theta \tag{15}$$

θ_0 and ϕ_0 are, respectively, the zenith and azimuth angles of a vector from the point on the sea surface under a pixel to the sun.

θ and ϕ are, respectively, the zenith and azimuth angle of a vector from the pixel to the sensor.

$\omega_{Rayleigh}(\lambda)$ is the single scattering albedo of Rayleigh, usually $\omega(\lambda) = 1.0$.

$\tau_{Rayleigh}(\lambda)$ is the optical thickness of Rayleigh.

$$p_{Rayleigh}(\theta,\vartheta_0,\lambda) = P_{Rayleigh}(\theta_-,\lambda) + [\rho(\theta) + \rho(\theta_0)]P_{Rayleigh}(\theta_+,\lambda) \tag{16}$$

$\rho(\alpha)$ is Fresnel reflectance of the interface for an incident angle α, it is not relative to wavelength.

$P_{Rayleigh}(\alpha,\lambda)$ is scattering phase function of Rayleigh at λ.

$$P_{Rayleigh}(\alpha,\lambda) = \frac{3}{4}(1 + \cos^2\alpha) \tag{17}$$

So, we have $P_{Rayleigh}(\theta_-,\lambda) = \dfrac{3}{4}(1 + \cos^2\theta_-)$ \hfill (18)

and $P_{Rayleigh}(\theta_+,\lambda) = \dfrac{3}{4}(1 + \cos^2\theta_+)$ \hfill (19)

$$\cos\theta_+ = +\cos\theta_0\cos\theta - \sin\theta_0\sin\theta\cos(\phi - \phi_0) \tag{20}$$

$$\cos\theta_- = -\cos\theta_0\cos\theta - \sin\theta_0\sin\theta\cos(\phi - \phi_0) \tag{21}$$

It means that $p_{Rayleigh}(\theta,\vartheta_0,\lambda)$ actually depends on only angles (θ_0 and ϕ_0, θ and ϕ).

$F_0'(\lambda)$ is the instantaneous extraterrestrial solar irradiance, which is $E_0(\lambda)\delta_{ES}$ reduced by two trips through the ozone layer,

$$F_0'(\lambda) = E_0(\lambda)\delta_{ES}e^{-\tau_{Oz}(1/\cos\theta + 1/\cos\theta_0)}$$

where $\tau_{Oz}(\lambda)$ is the ozone optical thickness.

Thus, $\dfrac{\pi \cdot L_{Rayleigh}(\lambda)}{E_0(\lambda)\delta_{ES}\cos\theta_0}$ is given by

$$\frac{\pi}{E_0(\lambda)\delta_{ES}\cos\theta_0} \cdot \frac{\tau_{Rayleigh}(\lambda)E_0(\lambda)\delta_{ES}\left[P_{Rayleigh}(\theta_-,\lambda) + \left(\rho(\theta) + \rho(\theta_0)\right)P_{Rayleigh}(\theta_+,\lambda)\right]}{e^{\tau_{Oz}(1/\cos\theta + 1/\cos\theta_0)}4\pi\cos\theta} \tag{22}$$

$$= \frac{\tau_{Rayleigh}(\lambda)\left[P_{Rayleigh}(\theta_-,\lambda) + \left(\rho(\theta) + \rho(\theta_0)\right)P_{Rayleigh}(\theta_+,\lambda)\right]}{e^{\tau_{Oz}(1/\cos\theta + 1/\cos\theta_0)}4\cos\theta\cos\theta_0} \tag{23}$$

As a summary,

$$R(\lambda) = \frac{1}{T_2(\lambda)} \left[\frac{\pi \cdot L_{sensor}(\lambda)}{E_0(\lambda)\delta_{ES}\cos\theta_0} - \frac{\tau_{Rayleigh}(\lambda)\left[P_{Rayleigh}(\theta_-,\lambda) + (\rho(\theta) + \rho(\theta_0))P_{Rayleigh}(\theta_+,\lambda)\right]}{e^{\tau_{Oz}(1/\cos\theta + 1/\cos\theta_0)}4\cos\theta\cos\theta_0} \right] (24)$$

$T_2(\lambda) = e^{-\left(\frac{\tau_{Rayleigh}}{2} + \tau_{Oz}\right)\left(\frac{1}{\cos\theta} + \frac{1}{\cos\theta_0}\right)}$ is the diffuse transmittance of the atmosphere on two trips between the sea surface and the sensor, and between the sea surface and the sun. The leading term in the brackets of Equation 24 includes $E_0(\lambda)$, which is in-band solar irradiance at the top of the atmosphere at the time of imaging. The succeeding term, however, does not includes $E_0(\lambda)$. This should be paid attention when analyzing the legacy codes, because when calibrating AVHRR counts, some algorithms generate radiance received by sensor while others generate albedo at the top of the atmosphere. The first term actually is the albedo at the top of the atmosphere at imaging time. Under assumption of diffuse surfaces, albedo is equal to π*radiance. The second is the Rayleigh reduction at imaging time.

In the legacy codes, $\tau_{Rayleigh}$ and ρ are assigned empirical constants. For example, $\tau_{Rayleigh}$ is set to 0.051 and 0.022, τ_{Oz} is set to 0.035 and 0.090 for NOAA-12 channels 1 and 2, respectively. The $\rho(\theta)$ =0.022 for the satellite zenith angle, and $\rho(\theta_0)$ =0.03 for the sun zenith angle.

Solar Angles Calculation

When the imaging date and time are known, the zenith and azimuth angles of the Sun are given by Woolard and Clemence (1966) as follow:

$$\cos Z = \sin\delta_S \sin\varphi + \sin\delta_S \cos\varphi \cos t_h \qquad (25)$$

$$\sin Z \sin A = -\cos\delta_S \sin t_h \qquad (26)$$

where Z is solar zenith angle, A is solar azimuth angle (calculated clockwise from the North), φ is the latitude of the pixel, δ_S is the declination of the Sun (related to the imaging date), t_h is the hour angle of the Sun (related to the imaging time). δ_S changes from day to day and t_h changes with time through the day.

$$\delta_S = 23.45\frac{\pi}{180}\sin\left(2\pi\frac{\text{Julian\_day} + 284}{365.25}\right) \qquad (27)$$

Hour Angle = 15 * (12 – the current hour of the day)

The Hour Angle is the angular distance that the earth has rotated in a day. It is equal to 15 degrees multiplied by the number of hours from local solar noon. It is positive during the morning, reduces to zero at solar noon and becomes increasingly negative as the afternoon progresses.

Sensor Viewing Angles Calculation

Sensor viewing geometry is calculated based on map projection so it could be calculated by pixel location and satellite orbital parameters (Niu et al. 2001).
Based on sensor viewing geometry

$$\frac{\sin\beta}{R} = \frac{\sin(\pi - \eta)}{R + h} \qquad (28)$$

where η is the viewing zenith angle, β is the scan angle, R is the Earth's radius, and h is the satellite altitude. The scan angle of a pixel is given by:

$$\beta = \frac{|c - 1024|}{1024}V \qquad (29)$$

where c is the pixel's column, V is a half (one side) of field-of-view which is about 55^0.

Sensor viewing azimuth angle is calculated by Mercator projection. The Mercator projection is a cylindrical map projection. It is a conformal projection. The following equations determine the x and y coordinates of a point on a Mercator map from its latitude φ and longitude λ (with λ₀ being the longitude in the center of map):

$$x = \lambda - \lambda_0 \tag{30}$$

$$y = \ln\left(\tan\left(\frac{\pi}{4} + \frac{\varphi}{2} \right) \right) = \frac{1}{2} \ln\left(\frac{1 + \sin(\varphi)}{1 - \sin(\varphi)} \right) = \ln\left(\tan(\varphi) + \sec(\varphi) \right) \tag{31}$$

The scale is proportional to the secant of the latitude φ, becoming arbitrarily large near the poles, where $\varphi = \pm 90°$.

Roughly, a scan line can be assumed to have one azimuth angle. Each scan line has 40 Earth location points, each with latitude and longitude. The 10th and 30th Earth location points are projected onto a Mercator projection plane for (x_0, y_0) and (x_1, y_1). The viewing azimuth α is given by:

$$\alpha = \tan \frac{y_1 - y_0}{x_1 - x_0} \tag{32}$$

According to the scan direction, α should be adjusted so that it represents clockwise from the North.

FUTURE WORKS

The latitude and longitude of points provided by a HRPT file has up to several kilometers of location accuracy. This low accuracy hinders extensive use of AVHRR data, particularly in area close to shore. Georeferencing, therefore, is an important issue for future work.

REFERENCES

Stumpf, R.P. 1988, Satellite detection of bloom and pigment distributions in estuaries, *Remote Sensing of Environment*, 24:385-404.

Heidinger, K. Andrew, W. C. Straka, C. C. Molling, J. T. Sullivan, and X. Wu, 2010. Deriving an inter-sensor consistent calibration for the AVHRR solar reflectance data record. *International Journal of Remote Sensing*, 31(24):6493-6517.

Gordon, H. R. and D. J. Castano, 1987. Coastal Zone Color Scanner atmospheric correction algorithm: multiple scattering effects, *Applied Optics*, 26(11): 2111-2122.

Gordon, H. R. , J. W. Brown, and R. H. Evans, 1988. Exact Rayleigh scattering calculations for use with the Nimbus-7 Coastal Zone Color Scanner. *Applied Optics*, 27(5):862-871.

Stumpf, R. P. and J. R. Pennock, 1989. Calibration of a General Optical Equation for Remote Sensing of Suspended Sediments in a Moderately Turbid Estuary. *Journal of Geophysical Research*, 94(C10):14,363-14,371.

Rao, C., R. Nagaraja, and J. Chen, 1996. Post-launch calibration of the visible and near-infrared channels of the Advanced Very High Resolution Radiometer on the NOAA-14 spacecraft, *International Journal of Remote Sensing*, 17:14, 2743-2747

RAO, C., R. Nagaraja, and J. Chen, 1995. Inter-satellite calibration linkages for the visible and nearinfared channels of the Advanced Very High Resolution Radiometer on the NOAA-7, -9, and -11 spacecraft, *International Journal of Remote Sensing*, 16(11):1931-1942.

Tahnk, W.R. and J. A. Coakley Jr., 2002. Improved Calibration Coefficients for NOAA-12 and NOAA-15 AVHRR Visible and Near-IR Channels. *Journal of Atmospheric and Oceanic Technology*, 19:11,1826-1,833.

Niu, Z., C. Y. Wang, W. Wamg, Q. Y. Zhang, and S. S. Young, 2001. Estimating bi-directional angles in NOAA AVHRR images. *International Journal of Remote Sensing*. 22(8):1,609-1,615.